Hindawi Publishing Corporation
Journal of Nanomaterials
Volume 2013, Article ID 797082, 8 pages
http://dx.doi.org/10.1155/2013/797082

Research Article

3D $Cu(OH)_2$ Hierarchical Frameworks: Self-Assembly, Growth, and Application for the Removal of TSNAs

Hongwei Hou,[1] You Zhu,[2] and Qingyuan Hu[1]

[1] *China National Tobacco Quality Supervision & Test Center, No. 2 Fengyang Street, Zhengzhou High & New Technology Industries Development Zone, Zhengzhou 450001, China*
[2] *Shandong Tobacco Quality Supervision and Testing Station, Xinluo Street, High & New Technology Industries Development Zone, Jinan 250101, China*

Correspondence should be addressed to Hongwei Hou; houhw@ztri.com.cn and Qingyuan Hu; huqy@ztri.com.cn

Received 25 March 2013; Accepted 7 May 2013

Academic Editor: Zhenhui Kang

The 3D hierarchical $Cu(OH)_2$ frameworks were successfully prepared via a simple and surfactant-free chemical self-assembled route. The frameworks were characterized by X-ray powder diffraction, field-emission scanning electron microscopy, and energy dispersive X-ray spectroscopy. The experimental investigations suggest that certain concentrations of NaOH and $K_2S_2O_8$ are required for the self-assembly and growth of $Cu(OH)_2$. In addition, the orthorhombic crystal structure of $Cu(OH)_2$ may prove to be ideal for the structural development of the final 3D $Cu(OH)_2$ hierarchical frameworks. The nitrogen adsorption and desorption measurements indicate that the $Cu(OH)_2$ frameworks possess a Brunauer-Emmett-Teller surface area of approximately 163.76 $m^2\,g^{-1}$. Barrett-Joyner-Halenda measurement of the pore size distribution, as derived from desorption data, presented a distribution centered at 3.05 nm. Additionally, 10 mg of the $Cu(OH)_2$ framework can remove 47% of the N-nitrosonornicotine and 53% of the 4-(methylnitrosamino)-1-(3-pyridyl)-1-butanone in cigarette smoke. These results indicate that the $Cu(OH)_2$ frameworks may be a potential adsorbent for removing tobacco-specific N-nitrosamines (TSNAs) from cigarette smoke.

1. Introduction

Self-assembled materials are the building blocks of the 21st century just as alloys, plastics, and semiconductors are the building blocks of the 20th century. These materials are formed by interatomic and intermolecular interactions other than the traditional covalent, ionic, and metallic bonding forces [1]. Opportunities offered by self-assembled materials are becoming a significant factor in current research directions. Biological life forms demonstrate an intricate pattern of macroscopic structures and functions formed through a hierarchical series of forces. A consequence of this "intelligent self-assembly" is the functional utility of self-replication and self-repair.

Until recently, the application of self-assembly to build inorganic structures with morphological diversity and complexity of natural minerals reflects a remarkable level of control over high-order organization of inorganic materials [2–4]. In the process, surfactant, as an important control factor, has been widely used [5–7]. This generally introduced heterogeneous impurities and limited the application and further research of inorganic materials due to trace surfactant absorption. Orthorhombic $Cu(OH)_2$ with layered structure has opened a new challenging field in chemistry, biotechnology, and materials science due to its potential applications in sensors [8, 9]. Meanwhile, the magnetic property of $Cu(OH)_2$, which is sensitive to the intercalation of molecular anions, has made the material a promising candidate for the preparation of copper-based biomineral, such as orthorhombic $Cu_2(OH)_3Cl$ [10, 11]. Inspired by the layered structure and its accompanying fundamental and practical applications, $Cu(OH)_2$ and the self-assembly synthesis of its elaborate morphologies have attracted considerable attention.

There is growing interest in the synthesis and morphological control of the $Cu(OH)_2$ nanoribbons, nanowires, nanotubes, and nanorods [12–23]. Despite the excellent approaches on the synthesis routes of low-dimensional $Cu(OH)_2$, only a few pieces of work on the 3D architectures of

$Cu(OH)_2$ have been reported. M. Y. Han's group reported the 3D nanoarchitectures of dendritic $Cu(OH)_2$ [23]. The oxygen from the atmosphere induced the spontaneous oxidation reaction of copper foil in the presence of formamide, and Cu^{2+} ions were released continuously from the copper foil into the formamide solution while oxygen was reduced. The released copper ions can be captured by coordinating with formamide molecules to form copper complexions ($Cu + 1/2O_2 + H_2O + 4HCONH_2 \rightarrow [Cu(HCONH_2)_4]^{2+} + 2OH^-$), which transformed into 3D dendritic copper hydroxide on substrate in 10 days.

The removal of tobacco-specific nitrosamines (TSNAs), N-nitrosonornicotine (NNN), 4-(methylnitrosamino)-1-(3-pyridyl)-1-butanone (NNK), N-nitrosoanatabine (NAT), and N-nitrosoanabasine (NAB) from cigarette smoke has attracted growing interest over the past years, because of the potent carcinogens in animal studies of TSNAs [24–26]. The design and preparation of new materials are crucial for removing carcinogenic compounds from tobacco smoke. However, to the best of our knowledge, the reduction of TSNAs in cigarette smoke using the 3D hierarchical $Cu(OH)_2$ frameworks has not been reported until now.

In this work, a fast and template-free approach for the progressive production of 3D hierarchical $Cu(OH)_2$ frameworks was developed from the oxidation of copper metal under a highly alkaline condition. The high-order, shell-ornamented, self-assembled structures keep the framework in the foreground of research in natural biominerals or synthetic materials. This unexplored $Cu(OH)_2$ frameworks with interesting morphologies and high surface area are the extension of the work of 3D epitaxial scrolls on the $Cu(OH)_2$ ribbons on the copper foil [14]. On the basis of a series of comparative experiments, the formation mechanism and the TSNAs reduction rate of the 3D $Cu(OH)_2$ hierarchical frameworks in cigarette smoke were proposed and thoroughly investigated. It is expected that the impressive 3D frameworks of $Cu(OH)_2$ might bring new ways to reduce carcinogenic compounds in cigarette smoke in the near future.

2. Experimental Methods

A typical synthesis of 3D $Cu(OH)_2$ hierarchical frameworks on copper foil was performed as follows: an aqueous solution was prepared in a 50 mL glass bottle by mixing 8.4 g of NaOH (7 mol L^{-1}), 1.08 g of $K_2S_2O_8$ (0.13 mol L^{-1}), and 30 mL of water that were analytically pure. A piece of 99.99% copper foil ($5 \times 2.5 \times 0.25$ mm^3), which was cleaned in 30% nitric acid for 20 s, rinsed in deionized water and ultrasonically cleaned in acetone, was immersed in the solution. After 30 min, the copper foil was taken out of the solution and rinsed with distilled water.

The phase identification of the samples was carried out using X-ray powder diffraction (XRD) patterns with a MAC Science Co. Ltd. MXP 18 AHF X-ray diffractometer with Cu Kα radiation (λ = 1.54056 Å). The morphology of the products was in situ measured by scanning electron microscopy (FE-SEM JEOL JSM-6700F, FEI PHILIPS XL30 ESEM-TMP) and energy dispersive X-ray spectroscopy

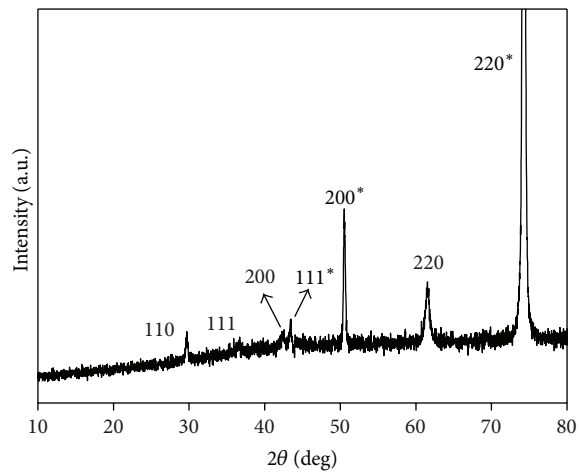

Figure 1: XRD pattern of the as-prepared sample with [NaOH] = 7 mol L^{-1} and [$K_2S_2O_8$] = 0.13 mol L^{-1} for 30 min (peaks marked with "*" correspond to the copper foil).

(EDS OXFORD INCA400). The nitrogen adsorption and desorption isotherms at 77 K were measured with a Micrometrics ASAP 2020 analyzer. Before measurement, the samples were degassed in vacuum at 140°C for at least 6 h.

The content of TSNAs in cigarette smoke was analyzed by liquid chromatography with tandem mass spectrometry (LC-MS/MS, API 5500 triple quadruple mass spectrometer, Applied Biosystems, Foster City, CA, USA). For the wet cut tobacco, a certain amount of $Cu(OH)_2$ hierarchical frameworks was dispersed in water to form an emulsion with a concentration of 50 g L^{-1}. Subsequently, the cut tobacco was sprayed with different volumes of emulsion to obtain 10 mg $cigarette^{-1}$. The wet cut tobacco samples were dried at 40°C until the moisture content was approximately 12%. The cut tobacco treated by this method was used to make cigarettes with an automated process, and the final weight was 850 ± 30 mg. Before smoking, the cigarettes were conditioned at 295 ± 1 K and 60 ± 2% relative humidity for 48 h and then smoked by a Cerulean SM 450 smoking machine under the standard ISO regime (ISO 4387).

3. Results and Discussion

The composition of the sample was examined by X-ray diffraction (XRD). A typical XRD pattern of the sample is shown in Figure 1. All of the diffraction peaks can be indexed to the orthorhombic phase $Cu(OH)_2$ (space group $Cmc2_1$, JCPDS card No. 13-420) except those marked with an "*", which were from the copper substrate.

The panoramic morphology of the sample, as examined by scanning electron microscopy and shown in Figure 2(a), indicated that the hierarchical framework with spherulitic texture grew onto the copper surface. Single particles had a round shape and a uniform size of 10 μm, and peanut- or dumbbell-like particles were formed when two particles merged together. Other shapes were also produced when three or more particles fused together. The structure and

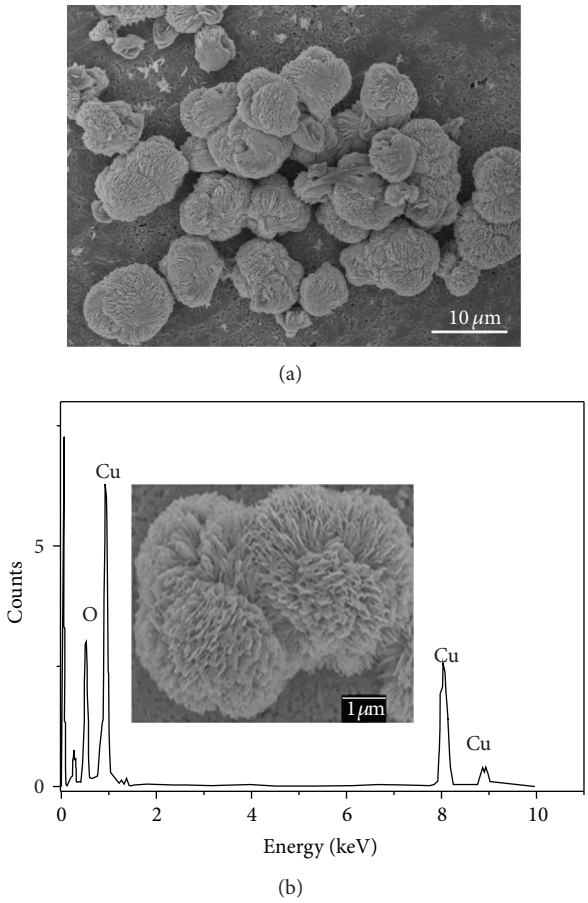

Figure 2: (a) FESEM image of the 3D $Cu(OH)_2$ hierarchical framework prepared with [NaOH] = 7 mol L^{-1} and [$K_2S_2O_8$] = 0.13 mol L^{-1} for 30 min. (b) EDS analysis of the hierarchical framework.

composition of the hierarchical framework was characterized by energy dispersive X-ray spectroscopy (EDS) as shown in Figure 2(b). The appropriate molar ratio of Cu : O = 1 : 2, which confirmed well to the XRD results.

The images of a typical single framework are shown in Figures 3(a) and 3(b), which indicated a flower-like morphology with lamellar and hierarchical structure. The magnified 3D spherical morphology confirmed that the highly porous structure with ultrathin lamellar structures of ~25 nm in thickness was identical throughout the hierarchical crystal. Figure 3(c) shows the submicrometer $Cu(OH)_2$ structures prepared in a previous study with [KOH] = 2.5 mol L^{-1} and [$K_2S_2O_8$] = 0.13 mol L^{-1} for 15 min at 40°C [14]. The products on the ribbons were $Cu(OH)_2$ epitaxial scrolls. Furthermore, from the magnified images shown in Figure 3(d), these submicrometer structures were wool balls growing from the ribbons and formed from the lamellar structures. The difference in concentration of alkalinity and $K_2S_2O_8$ was the sole contributing factor for the different morphologies in the as-prepared samples. This observation suggested that an appropriate concentration of alkalinity and $K_2S_2O_8$ was essential to the unique and interesting morphology.

In the present approach, the formation of $Cu(OH)_2$ on copper foil involved a simple oxidation process described as follows:

$$\mathrm{Cu} + 2\ \mathrm{NaOH} + \mathrm{K_2S_2O_8} \longrightarrow \mathrm{Cu(OH)_2} + \mathrm{Na_2SO_4} + \mathrm{K_2SO_4} \quad (1)$$

It is well known that in order to attain the desired self-assembled structures, the effect of salts and ionic species in the system cannot be ignored [27]. This also suggests that a certain level of NaOH and $K_2S_2O_8$ concentration was required for the growth of the self-assembled $Cu(OH)_2$ hierarchical framework.

To thoroughly investigate the formation mechanism of the $Cu(OH)_2$ hierarchical framework, the influence of the concentrations of NaOH and $K_2S_2O_8$ to the $Cu(OH)_2$ morphology was examined. The $Cu(OH)_2$ samples produced under different concentrations of NaOH with [$K_2S_2O_8$] = 0.13 mol L^{-1} for 30 min were observed by SEM as shown in Figures 4(a)–4(d). At a lower concentration of [NaOH] = 0.13 mol L^{-1}, the oxidation process was slow and the final product was a few multiped crystals on the foil. When [NaOH] = 1 mol L^{-1}, many ribbons emerged. When [NaOH] = 3 mol L^{-1}, the products were some flower-like structures scrolled on the ribbons. After the concentration of NaOH was increased to 9 mol L^{-1}, the bulk crystals appeared on the foil. Similarly, the $Cu(OH)_2$ samples produced under different concentrations of $K_2S_2O_8$ with [NaOH] = 7 mol L^{-1} for 30 min were examined and the corresponding SEM images are shown in Figure 5. At a lower $K_2S_2O_8$ concentration of 0.033 mol L^{-1}, a mass of acicular crystals formed on the Cu foil as shown in Figures 5(a) and 5(b). When [$K_2S_2O_8$] = 0.17 mol L^{-1}, some scrolling floccule structures appeared and scrolled on the ribbons, as shown in Figures 5(c) and 5(d).

A comparison of the FESEM images of the $Cu(OH)_2$ structures prepared under different reaction times with [NaOH] = 7 mol L^{-1} and [$K_2S_2O_8$] = 0.13 mol L^{-1} showed that the oxidation process was fast. Namely, the high alkalinity and the effect of the oxidant determined the rapid rate of growth. Through the careful analysis of the samples produced under different reaction times, a possible growth process may be proposed. Under the initial high alkalinity, the copper foil oxidized expeditiously and produced crystals with a prism-like morphology (Figure 6(a)). After 5 min, many spindle-like, multiped crystals were found, as shown in Figure 6(b), which were 500 nm in length on average and consisted of several nanoribbons. Spindle-like structures have been validated as one of the structures of hydroxide [28]. As the reaction proceeded, the coherent nanoribbons began curving as shown in Figure 6(c). After 15 min, the straight nanoribbons were edged out by curved ones (Figure 6(d)). After 20 min, the outline of the structures was finalized with a much smaller size (Figure 6(e)). Then at 30 min, the 3D hierarchical framework formed, as shown in Figure 6(f).

Based on the above discussions of $Cu(OH)_2$ morphology, the orthorhombic crystal structure of $Cu(OH)_2$ may prove to be ideal for the development of the final $Cu(OH)_2$ structure

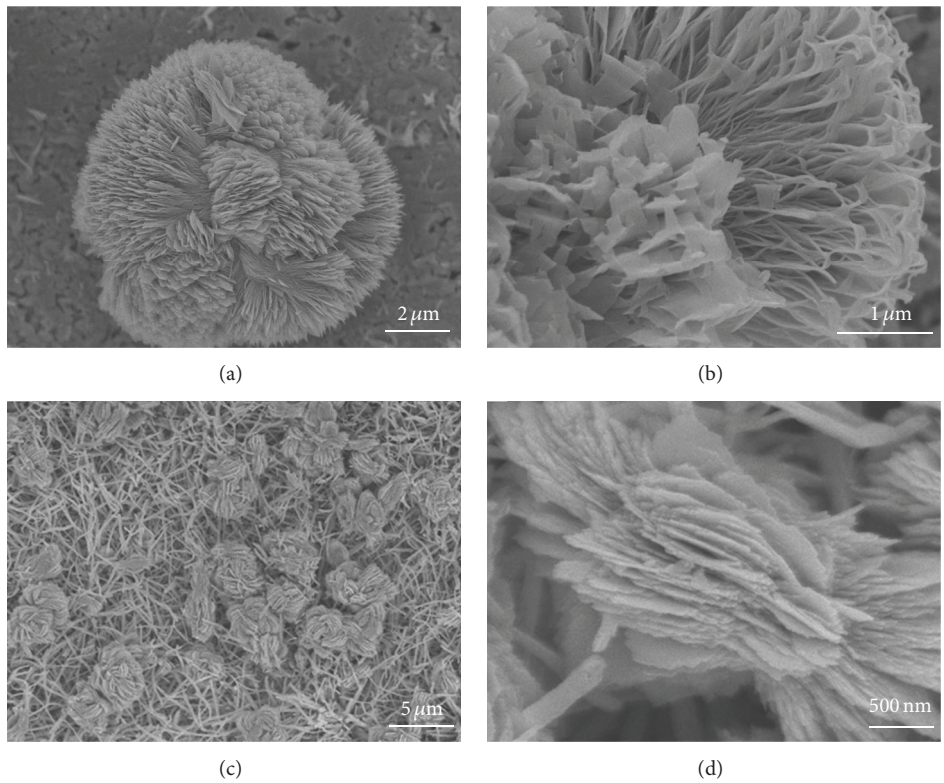

Figure 3: ((a), (b)) FESEM image of the 3D $Cu(OH)_2$ hierarchical framework with [NaOH] = 7 mol L^{-1} and [$K_2S_2O_8$] = 0.13 mol L^{-1} for 30 min. ((c), (d)) FESEM image of the $Cu(OH)_2$ scrolling structures on the $Cu(OH)_2$ submicrometer ribbons with [KOH] = 2.5 mol L^{-1} and [$K_2S_2O_8$] = 0.13 mol L^{-1} for 15 min at 40°C.

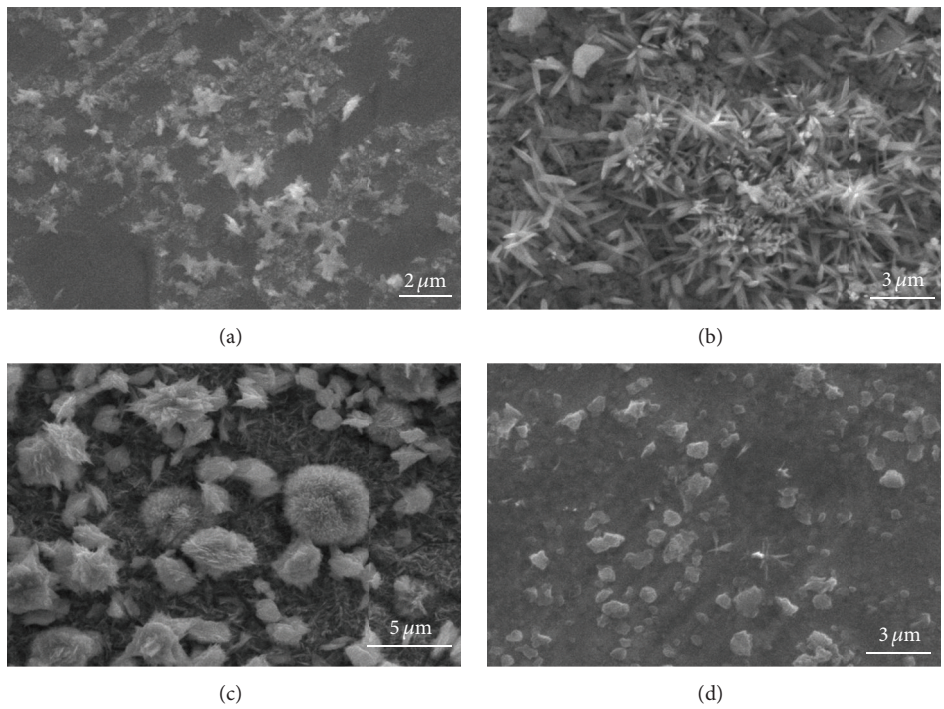

Figure 4: FESEM images of $Cu(OH)_2$ structures prepared under different concentrations of NaOH with [$K_2S_2O_8$] = 0.13 mol L^{-1} for 30 min. (a) [NaOH] = 0.13 mol L^{-1}; (b) [NaOH] = 1 mol L^{-1}; (c) [NaOH] = 3 mol L^{-1}; (d) [NaOH] = 9 mol L^{-1}.

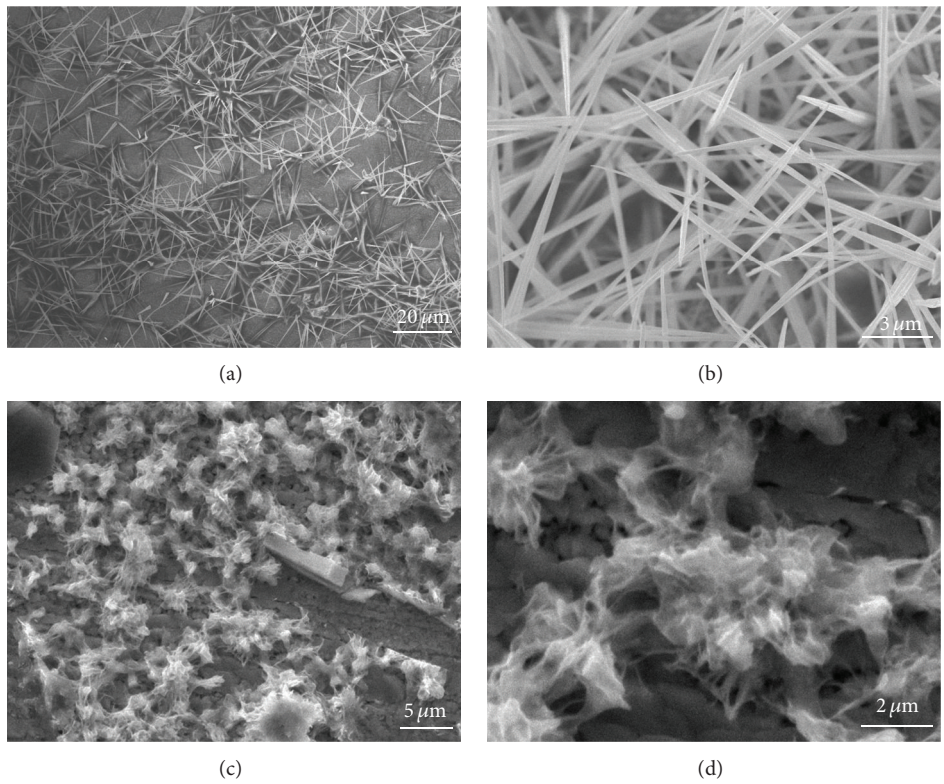

FIGURE 5: FESEM images of $Cu(OH)_2$ structures prepared under different concentrations of $K_2S_2O_8$ with [NaOH] = 7 mol L^{-1} for 30 min. ((a), (b)) [$K_2S_2O_8$] = 0.033 mol L^{-1}; ((c), (d)) [$K_2S_2O_8$] = 0.17 mol L^{-1}.

[29], as demonstrated by Huang [30–32]. In the process, the rapid rate of nucleation resulted in the small concentration of nucleus, which provided the possibility of anisotropic nuclear growth and determined the structure of $Cu(OH)_2$. The schematic illustration of the proposed development of the $Cu(OH)_2$ structure is shown in Figure 7. It is known that Cu^{2+} ions prefer square planar coordination by OH^- (shown in Figure 7(a)), which leads to an extended chain (Figure 7(b)). The chains can be connected through the coordination of OH^- to dz^2 of Cu^{2+}, forming two-dimensional (2D) ultrathin sheet-like structures (Figure 7(c)). Finally, the 2D layers are stacked through the relatively weak hydrogen bond interactions, and two or more adjacent hierarchical crystals can further expand and eventually self-organize/merge into continuous porous networks [33, 34] and an intricate three-dimensional (3D) crystal (Figure 7(d)).

The self-assembly process involves forces such as hydrogen bonding, dipolar forces, other van der Waals forces, hydrophilic or hydrophobic interactions (all frequently referred to as "supramolecular interactions"), chemisorption, surface tension, and gravity. Forces involving ions and ligands (the "coordinate-covalent bond") have resulted in supramolecular structures [12]. Considering the related experimental results and the possible development of $Cu(OH)_2$ structure, we predict that a certain level of concentration of NaOH and $K_2S_2O_8$ is required for the self-assembly and growth of $Cu(OH)_2$, and the lamellar structure of $Cu(OH)_2$ is the determining factor for the final hierarchical framework. That is, the potential self-assembly forces in $Cu(OH)_2$ will induce the formation of the 3D hierarchical framework under the appropriate concentration of NaOH and $K_2S_2O_8$. Using experimental results, we propose the possible mechanism for the assembly and growth of the $Cu(OH)_2$ hierarchical framework. After the initial nucleation, the newly formed $Cu(OH)_2$ will grow into nanoparticles followed by the formation of primary, radical, and spindle-like multiped structures (as shown in Figure 6) as the result of the anisotropic nature of the $Cu(OH)_2$ structure. Under the appropriate levels of NaOH and $K_2S_2O_8$, the copper foil will be further eroded while making the $Cu(OH)_2$ structure evolve rapidly from the lamellar structure to the 3D hierarchical framework. Namely, the spindle-like multiped structures will continue to fissure and grow, driven by the self-assembly forces as mentioned earlier [35, 36].

Nitrogen adsorption/desorption measurements were conducted to characterize the Brunauer-Emmett-Teller (BET) surface area and internal pore structure. The recorded adsorption and desorption isotherms for the 3D $Cu(OH)_2$ hierarchical frameworks are shown in Figure 8. The BET specific surface area of the sample was calculated from N_2 isotherms to be approximately 163.76 m^2 g^{-1}. Barrett-Joyner-Halenda (BJH) measurements for the pore-size distribution, as derived from desorption data, presented a distribution centered at 3.05 nm. The smaller pores presumably arose

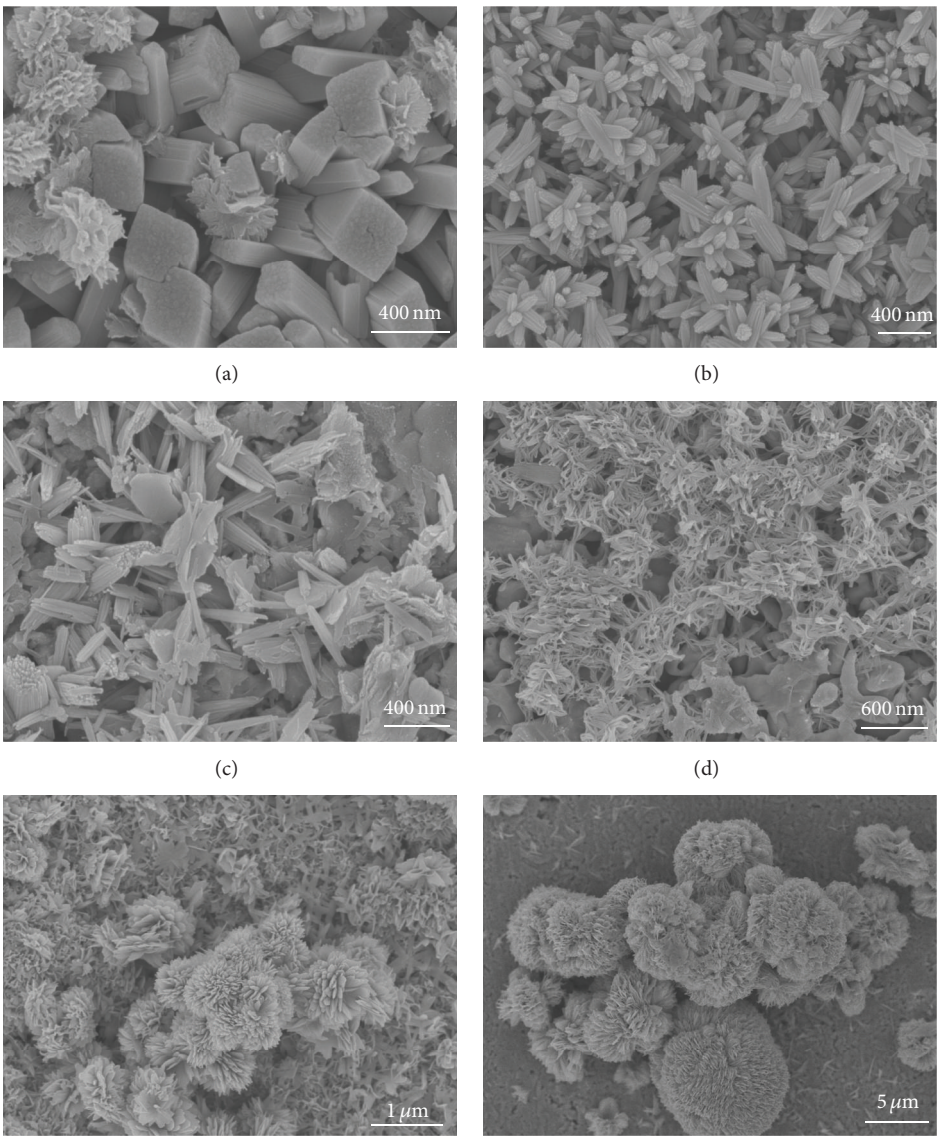

Figure 6: FESEM images of the $Cu(OH)_2$ structures prepared with [NaOH] = 7 mol L^{-1} and $[K_2S_2O_8]$ = 0.13 mol L^{-1} for (a) 1 min, (b) 5 min, (c) 10 min, (d) 15 min, (e) 20 min, and (f) 30 min.

Table 1: The amount of four TSNAs in cigarette smoke produced by cut tobacco with the 3D $Cu(OH)_2$ hierarchical framework.

Compounds		Blank cigarette*	10 mg cigarette^{-1} 3D $Cu(OH)_2$	Reduction (%)
NNN	ng cig^{-1}	49.56	26.25	47
NAT		28.22	20.35	28
NAB		15.21	11.56	24
NNK		18.20	8.62	53
Tar	mg cig^{-1}	13.50	12.80	5

*The blank cigarette was identical to the one with no $Cu(OH)_2$.

from the spaces within the hierarchical structure. The results showed that the obtained hierarchical frameworks were porous and confirmed well with the FESEM images.

The as-prepared 3D $Cu(OH)_2$ hierarchical frameworks were wetted and put into the cut tobacco to study the TSNAs content in cigarette smoke. Table 1 shows the content of four TSNAs in cigarette smoke after adding 3D $Cu(OH)_2$ hierarchical frameworks into cut tobacco, which was analyzed by LC-MS/MS. Compared with "blank" cigarettes with no 3D $Cu(OH)_2$, the TSNAs contents of cigarettes with

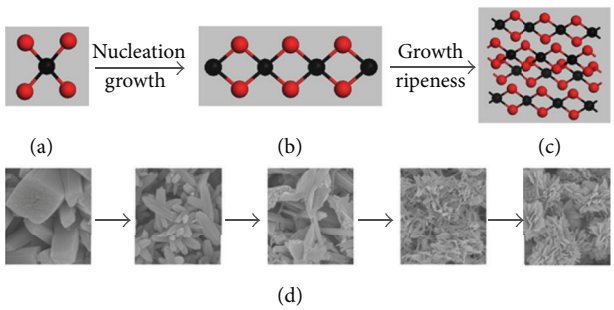

FIGURE 7: Schematic illustration of the proposed development of the $Cu(OH)_2$ structure. (a) The layered structure of orthorhombic $Cu(OH)_2$, (b) further growing of layered structure, (c) formation of a two-dimensional (2D) ultrathin sheet-like structure; (d) the whole growth process of self-assembling and ripening of the 3D $Cu(OH)_2$ hierarchical framework.

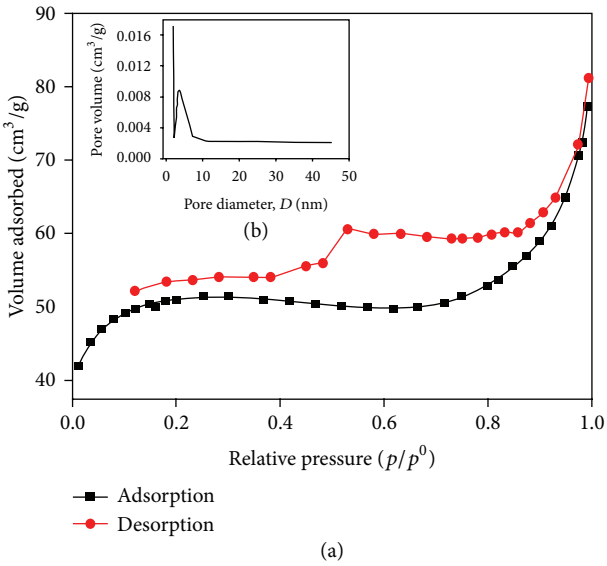

FIGURE 8: N_2 absorption and desorption isotherms and pore size distribution (inset) for the 3D $Cu(OH)_2$ hierarchical framework.

10 mg cigarette^{-1} $Cu(OH)_2$ were selectively reduced with no changes in tar content, which may influence the cigarette smoke quality. The adsorptive capacity of $Cu(OH)_2$ for NNN, NAT, NAB, and NNK is 47%, 28%, 24%, and 53%, respectively. Because the $Cu(OH)_2$ could block the N–NO group and hamper the formation of TSNAs [25], the 3D $Cu(OH)_2$ hierarchical framework added into the cut tobacco not only influenced cigarette combustion, but also worked as adsorbents that reduce the amount of TSNAs. When $Cu(OH)_2$ with sophisticated morphology was added into the wet tobacco, chemical transitions took place during burning and showed to be more effective than zeolite.

A cigarette sample added $Cu(OH)_2$ frameworks and a blank sample (with no $Cu(OH)_2$ frameworks) were smoked under the standard ISO regime (ISO 4387). Toxicology tests including cytotoxic test, mutagenicity testing of salmonella typhimurium, and in vitro micronucleus test were used to detect the influence of health. The three smoke toxicology tests showed that there were no significant differences between the two samples.

4. Conclusions

A template-free, chemical route involving a simple oxidation process to grow self-assembled 3D $Cu(OH)_2$ hierarchical frameworks was developed. In comparison with other approaches, the alternative route is fast, safe, simple, and inexpensive and this effective and convenient method is suitable for modern chemical synthesis of 3D hierarchical frameworks. The experimental investigations suggest that certain concentrations of NaOH and $K_2S_2O_8$ are required for the self-assembly and growth of $Cu(OH)_2$. Furthermore, the orthorhombic crystal structure of $Cu(OH)_2$ may prove to be ideal for the structural development of the final $Cu(OH)_2$ hierarchical frameworks. The BET specific surface area of the sample was calculated from N_2 isotherms to be approximately 163.76 $m^2\,g^{-1}$. The BJH for the pore-size distribution presented a distribution centered at 3.05 nm. It was found that 10 mg of $Cu(OH)_2$ framework can remove 47% of the NNN and 53% of the NNK in cigarette smoke. The successful fabrication of the hierarchical morphology provides new applications in reducing the carcinogenic compounds in cigarette smoke.

Acknowledgments

Financial support from the National Natural Science Foundation of China (no. 20701040) is gratefully acknowledged. The authors thank the Hefei National Laboratory for Physical Sciences at the Microscale as well as the University of Science and Technology of China for the assistance with structural characterization.

References

[1] W. M. Tolles, "Self-assembled materials," *MRS Bulletin*, vol. 25, no. 10, pp. 36–38, 2000.

[2] J. Aizenberg, A. Tkachenko, S. Weiner, L. Addadi, and G. Hendler, "Calcitic microlenses as part of the photoreceptor system in brittlestars," *Nature*, vol. 412, no. 6849, pp. 819–822, 2001.

[3] D. L. Beke, "On the composition and pressure dependence of the self-diffusion coefficient in liquid metals," *International Journal of Materials Research*, vol. 101, no. 3, pp. 353–355, 2010.

[4] R. K. Bortoleto-Bugs, T. Mazon, M. Tarozzo Biasoli, A. Pavani Filho, J. Willibrordus Swart, and M. Roque Bugs, "Understanding the formation of the self-assembly of colloidal copper nanoparticles by surfactant: a molecular velcro," *Journal of Nanomaterials*, vol. 2013, Article ID 802174, 8 pages, 2013.

[5] J. Texter, *Journal of DispersionScience and Technology*, vol. 22, no. 1, 5 pages, 2001.

[6] B. Russell, M. Payne, and L. C. Ciacchi, "Density functional theory study of Fe(II) adsorption and oxidation on goethite surfaces," *Physical Review B*, vol. 79, no. 16, Article ID 165101, 2009.

[7] A. Nazari and S. Riahi, "Physical and mechanical behavior of high strength self-compacting concrete containing ZrO_2 nanoparticles," *International Journal of Materials Research*, vol. 102, no. 5, pp. 560–571, 2011.

[8] W. Fujita and K. Awaga, "Reversible structural transformation and drastic magnetic change in a copper hydroxides intercalation compound," *Journal of the American Chemical Society*, vol. 119, no. 19, pp. 4563–4564, 1997.

[9] W. Fujita and K. Awaga, "Intercalation of stable organic radicals into layered copper hydroxides," *Synthetic Metals*, vol. 122, no. 3, pp. 569–572, 2001.

[10] H. C. Lichtenegger, T. Schöberl, M. H. Bartl, H. Waite, and G. D. Stucky, "High abrasion resistance with sparse mineralization: copper biomineral in worm jaws," *Science*, vol. 298, no. 5592, pp. 389–392, 2002.

[11] S. Weiner and L. Addadi, "Biomineralization: at the cutting edge," *Science*, vol. 298, no. 5592, pp. 375–376, 2002.

[12] X. Wen, W. Zhang, S. Yang, Z. R. Dai, and Z. L. Wang, "Solution phase synthesis of $Cu(OH)_2$ nanoribbons by coordination self-assembly using Cu_2S nanowires as precursors," *Nano Letters*, vol. 2, no. 12, pp. 1397–1401, 2002.

[13] W. Z. Wang, C. Lan, Y. Z. Li, K. Q. Hong, and G. H. Wang, "A simple wet chemical route for large-scale synthesis of $Cu(OH)_2$ nanowires," *Chemical Physics Letters*, vol. 366, no. 3-4, pp. 220–223, 2002.

[14] W. X. Zhang, X. G. Wen, and S. H. Yang, "Controlled reactions on a copper surface: synthesis and characterization of nanostructured copper compound films," *Inorganic Chemistry*, vol. 42, no. 16, pp. 5005–5014, 2003.

[15] X. Wen, W. Zhang, and S. Yang, "Synthesis of $Cu(OH)_2$ and CuO nanoribbon arrays on a copper surface," *Langmuir*, vol. 19, no. 14, pp. 5898–5903, 2003.

[16] W. Zhang, X. Wen, S. Yang, Y. Berta, and Z. L. Wang, "Single-crystalline scroll-type nanotube arrays of copper hydroxide synthesized at room temperature," *Advanced Materials*, vol. 15, no. 10, pp. 822–825, 2003.

[17] G. H. Du and G. Van Tendeloo, "$Cu(OH)_2$ nanowires, CuO nanowires and CuO nanobelts," *Chemical Physics Letters*, vol. 393, no. 1–3, pp. 64–69, 2004.

[18] X. Song, S. Sun, W. Zhang, H. Yu, and W. Fan, "Synthesis of $Cu(OH)_2$ nanowires at aqueous-organic interfaces," *Journal of Physical Chemistry B*, vol. 108, no. 17, pp. 5200–5205, 2004.

[19] C. Lu, L. Qi, J. Yang, D. Zhang, N. Wu, and J. Ma, "Simple template-free solution route for the controlled synthesis of $Cu(OH)_2$ and CuO nanostructures," *Journal of Physical Chemistry B*, vol. 108, no. 46, pp. 17825–17831, 2004.

[20] S.-H. Park and H. J. Kim, "Unidirectionally aligned copper hydroxide crystalline nanorods from two-dimensional copper hydroxy nitrate," *Journal of the American Chemical Society*, vol. 126, no. 44, pp. 14368–14369, 2004.

[21] P. Gao, M. Zhang, Z. Niu, and Q. Xiao, "A facile solution-chemistry method for $Cu(OH)_2$ nanoribbon arrays with noticeable electrochemical hydrogen storage ability at room temperature," *Chemical Communications*, no. 48, pp. 5197–5199, 2007.

[22] Y. Ni, H. Li, L. Jin, and J. Hong, "Synthesis of 1D $Cu(OH)_2$ nanowires and transition to 3D CuO microstructures under ultrasonic irradiation, and their electrochemical property," *Crystal Growth & Design*, vol. 9, no. 9, pp. 3868–3873, 2009.

[23] W. Jia, E. Reitz, H. Sun, H. Zhang, and Y. Lei, "Synthesis and characterization of novel nanostructured fishbone-like $Cu(OH)_2$ and CuO from $Cu_4SO_4(OH)_6$," *Materials Letters*, vol. 63, no. 5, pp. 519–522, 2009.

[24] K. A. Wagner, N. H. Finkel, J. E. Fossett, and I. G. Gillman, "Development of a quantitative method for the analysis of tobacco-specific nitrosamines in mainstream cigarette smoke using isotope dilution liquid chromatography/electrospray ionization tandem mass spectrometry," *Analytical Chemistry*, vol. 77, no. 4, pp. 1001–1006, 2005.

[25] Y. Zhu, H. W. Hou, G. L. Tang, and Q. Y. Hu, "Synthesis of three-quarter-sphere-like γ-AlOOH superstructures with high adsorptive capacity," *European Journal of Inorganic Chemistry*, no. 6, pp. 872–878, 2010.

[26] W. Xiong, H. Hou, X. Jiang, G. Tang, and Q. Hu, "Simultaneous determination of four tobacco-specific N-nitrosamines in mainstream smoke for Chinese Virginia cigarettes by liquid chromatography-tandem mass spectrometry and validation under ISO and "Canadian intense" machine smoking regimes," *Analytica Chimica Acta*, vol. 674, no. 1, pp. 71–78, 2010.

[27] Z. P. Zhang, X. Q. Shao, H. D. Yu, Y. B. Wang, and M. Y. Han, "Morphosynthesis and ornamentation of 3D dendritic nanoarchitectures," *Chemistry of Materials*, vol. 17, no. 2, pp. 332–336, 2005.

[28] H. Hou, Y. Xie, and Q. Li, "Large-scale synthesis of single-crystalline quasi-aligned submicrometer CuO ribbons," *Crystal Growth & Design*, vol. 5, no. 1, pp. 201–205, 2005.

[29] H. Hou, Y. Xie, Q. Yang, Q. Guo, and C. Tan, "Preparation and characterization of γ-AlOOH nanotubes and nanorods," *Nanotechnology*, vol. 16, no. 6, pp. 741–745, 2005.

[30] C.-C. Huang, C.-S. Yeh, and C.-J. Ho, "Laser ablation synthesis of spindle-like gallium oxide hydroxide nanoparticles with the presence of cationic cetyltrimethylammonium bromide," *Journal of Physical Chemistry B*, vol. 108, no. 16, pp. 4940–4945, 2004.

[31] L. C. Varanda, M. P. Morales, M. Jafelicci Jr., and C. J. Serna, "Monodispersed spindle-type goethite nanoparticles from FeIII solutions," *Journal of Materials Chemistry*, vol. 12, no. 12, pp. 3649–3653, 2002.

[32] T. Sugimoto, K. Okada, and H. Itoh, "Formation mechanism of uniform spindle-type titania particles in the gel-sol process," *Journal of Dispersion Science and Technology*, vol. 19, no. 2-3, pp. 143–161, 1998.

[33] Y. Cudennec and A. Lecerf, "The transformation of $Cu(OH)_2$ into CuO, revisited," *Solid State Sciences*, vol. 5, no. 11-12, pp. 1471–1474, 2003.

[34] R. Rodríguez-Clemente, C. J. Serna, M. Ocaña, and E. Matijević, "The relationship of particle morphology and structure of basic copper(II) compounds obtained by homogeneous precipitation," *Journal of Crystal Growth*, vol. 143, no. 3-4, pp. 277–286, 1994.

[35] F. J. Opalko, J. H. Adair, and S. R. Khan, "Heterogeneous nucleation of calcium oxalate trihydrate in artificial urine by constant composition," *Journal of Crystal Growth*, vol. 181, no. 4, pp. 410–417, 1997.

[36] K. Naka and Y. Chujo, "Control of crystal nucleation and growth of calcium carbonate by synthetic substrates," *Chemistry of Materials*, vol. 13, no. 10, pp. 3245–3259, 2001.